



Utrecht University

Granzyme B-Loaded Nanogels: A Novel Cancer Delivery System

Author: BSc JianXi Zhu

Supervisor: Dr.R.W. (Reece) Lewis

Referee: Dr.C.F. (Rene) van Nostrum

Examiner: Prof. Dr. N. (Niels) Bovenschen

Date: 08-11-2024

Course: FA-MA 203

Research institute: Department of Pharmaceutical Sciences

Research group: Pharmaceutics

University: Utrecht University

Table of contents

1. Abstract.....	3
2. Introduction	4
3. Methods	7
3.1 Materials	7
3.2 Synthesis and characterization of anionic nanogels	7
3.3 Protein loading	7
3.3a Protein content determination by Micro-BCA assay.....	8
3.3b Protein content determination by UPLC.....	8
3.4 Synthesis and characterization of cationic polymer coating	8
3.4a Synthesis of pyridyl disulfide incorporated-polycation (PD-PC)	8
3.4b Synthesis of ATAA incorporated polycation (ATAA-PC).....	9
3.5 Coating of anionic nanogel with cationic polymer	9
3.6 Cross-linking of coated anionic nanogel.....	9
3.7 In vitro release from coated nanogels	10
3.8 Fluorescence Correlation Spectroscopy study	10
4. Results and discussion.....	11
4.1 Synthesis and Characterization of Anionic Nanogel	11
4.2 Loading efficiency of protein in nanogel	12
4.3 Cationic polymer synthesis and characterization after coating nanogel.....	14
4.4 In vitro release study.....	18
4.5 Fluorescence correlation microscopy study	19
5. Conclusion	20
6. Supporting information	21
7. References	23

1. Abstract

Cancer remains one of the leading causes of death worldwide. Despite the widespread use and clinical effectiveness of traditional anti-cancer treatments, there are significant drawbacks in their use, such as their lack of specificity, toxicity, resistance to treatment and relapse in disease. Therefore, there is a need for alternative anti-cancer therapies that are more targeted to cancer and less toxic to the patient. Immunotherapy utilizes the immune system to selectively target cancer cells. Granzyme B (GrB), a serine protease secreted by cytotoxic T lymphocytes (CTL) and natural killer cell, induces apoptosis in cancer cells. This study aims to develop a drug delivery system for GrB, simulating the CTL-mediated transport to target cancer cells.

Nanogels were synthesized to serve as vehicles for GrB, by incorporating a negative charge on the nanogel, positively charged GrB can be loaded via electrostatic interactions. A polycation coating was synthesized to enable the loaded nanogel to enter the tumoral intracellular environment. This polycation coating contained protected thiol groups that could be deprotected, allowing formation of disulfide cross-links. The cross-linked structure retains GrB in the nanogel under physiological conditions and releases it in the reductive environment of the cell. Nanogels loaded with lysozyme as a model protein, as well as GrB, were characterized for size and zeta potential. Furthermore, loading studies, release studies and fluorescence correlation spectroscopy were performed.

Anionic nanogels were successfully synthesized and demonstrated the ability to load granzyme B (GrB) via electrostatic interactions. The polycation coating was also successfully synthesized and allowed the production of the coated nanogel for further study. Unexpectedly, the GrB appeared to release under physiological conditions. There was no observed triggered GrB release under reductive conditions. Fluorescence correlation spectroscopy was not performed due to GrB protein aggregation.

In conclusion, we successfully designed a delivery system that can effectively load GrB and feature a polymer coating mimicking CTL cell-mediated transport. Future studies need to be done to refine the polycation coating and analyze alternative methods to investigate the controlled release of GrB. Ultimately, enhancing the potential of this delivery system to offer a more effective and less toxic alternative for cancer patients.

2. Introduction

Cancer is one of the leading causes of death globally.^[1] There are ongoing issues in cancer treatment due to the complexity of the disease, its ability to develop drug resistance, the ability to metastasize and spread throughout the body to new sites. There are also off-target effects of cancer treatments (chemotherapy and radiotherapy) that are toxic and damaging to healthy cells.^[2] Drug resistance can occur during or before tumor cells are exposed to the drug. This can be caused by molecular modifications in the binding domain of tumor cells, rendering the drug unable to bind and interact with the tumor cells.^[3] Additionally, when conventional therapies such as surgery, chemotherapy and radiotherapy fail to eliminate all of the tumor cells, the remaining cancer cells are able to proliferate and trigger a recurrence of disease.^[2] In response to these complications, there is a need for more potent and selective alternatives that can improve the current anti-cancer therapies.

The hallmarks of cancer are essential for determining targets for anti-cancer therapies and are recognized as requirements for cancer growth and metastasis.^[4] One hallmark is cancer's ability to avoid immune destruction. Cancer cells can achieve this by downregulating the production of recognized cancer antigens, therefore disguising themselves as healthy cells within the system. They also achieve this by promoting immunosuppressive signals that cause immune resistance.^[5] Targeting antigen-presenting cell function or inhibiting immunosuppressive signals, can help treat cancer. Several immunotherapies have been approved by the US Food and Drug Administration (FDA) and the European Medicines Agency (EMA) for cancer management.^[6,7] These include immune checkpoint inhibitors, cytokine therapies, and cancer vaccines. Immunotherapy utilizes the natural protective immune mechanisms against cancerous cells to kill the cancerous cells selectively.

In solid tumors, there is a low presence of immune cells due to limited permeation into the tumor cells. Immune cells that are able to permeate into the solid tumor mass can then be suppressed by the tumor environment.^[8] A potential anti-cancer strategy may involve using the immune pro-apoptotic intermediates secreted physiologically by cytotoxic T lymphocytes (CTLs) in the tumor environment. Granzymes are a family of serine proteases that can induce apoptosis of cancer cells by cleaving target proteins.^[9] Granzyme B (GrB) is the most abundant of the five human granzymes, and it partakes in CTLs and natural killer (NK) – mediated cytotoxicity.^[8] In these processes, it is stored within cytotoxic granules with pore-forming protein perforin (Figure 1).^[10] Upon recognition of cancer cells, the granules are secreted, and GrB enters the cancer cell through pores made by perforin. Once GrB is internalized, it activates multiple cascades, such as the mitochondrial pathway of apoptosis, activation of caspases, and cleavage of pro-apoptotic proteins like BH3 interacting-domain death agonist (BID), leading to cancer cellular death. This could be a promising targeted immunotherapy approach due to its ability to induce multiple apoptosis pathways once inside the cancer cells, making it less susceptible to tumor resistance.

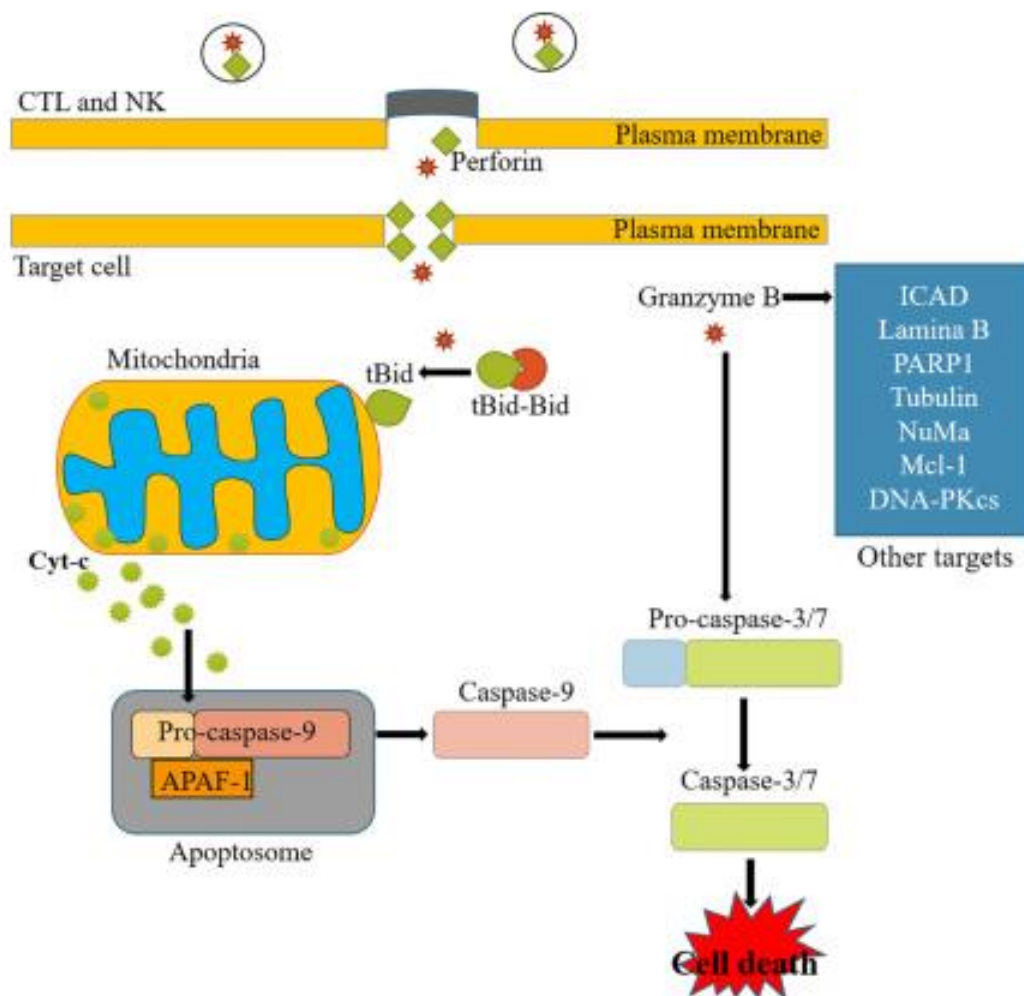


Figure 1. Mechanism of Granzyme B induced apoptosis. Granzyme B, synthesized by CTLs and NK cells, enters target cells via pores made by perforin. Inside the cell, Granzyme B induces apoptosis via the mitochondrial pathway and via activation of caspases-3/7.^[10]

For effective therapeutic use of GrB, it needs to be able to enter the tumor cells while maintaining stability under physiological conditions and only be released within the intracellular reductive environment of the tumor. Normally, perforin facilitates the entry of GrB into tumor cells.^[8] However, perforin is unstable and calcium-dependent, making it challenging to deliver exogenous GrB and perforin into tumor cells. A strategy could be by encapsulating GrB within nanogels enabling GrB to pass the cell membrane and enter the tumoral intracellular environment. Nanogels are three-dimensional nano-sized hydrogels with favorable properties that potentiate them as excellent protein delivery systems.^[11] For example, high protein loading and high biocompatibility due to their high-water content. Additionally, nanogels can protect their cargo from degradation by encapsulating proteins in their internal core and they also possess easily tunable physicochemical cross-linked structures. However, chemical nanogel crosslinking agents can have negative effects such as

chemical modification on the protein cargo which can lead to incomplete release when triggered.^[12] These problems can be overcome by loading the cargo protein post-nanogel synthesis. Previous research has shown that layer-by-layer coated nanogels can stably deliver the loaded proteins into the target cells.^[13] Coating the GrB-loaded nanogels with a stimuli-responsive cross-linkable polymer would ensure effective encapsulation and site-specific release. The stability of the nanogel in physiological conditions and release in the reducing environment is maintained by the reversibly cross-linking disulfide bonds.

This research project aims to mimic the CTL-mediated mechanism of action by developing a nanogel-based delivery system to vehiculate GrB (Figure 2). This system allows us to exploit the cytosol-reducing environment and use it as a stimulus to trigger the release of GrB after tumoral cell internalization. We will develop anionic dextran nanogels capable of post-loading the positively charged GrB via electrostatic interactions. These GrB-loaded nanogels will then be coated with a polycation containing protected thiols. Once coated, the thiols are deprotected to cross-link, forming disulfide cross-links. These disulfide cross-links can later be reduced in the reductive intracellular environment, releasing GrB into the tumor environment.

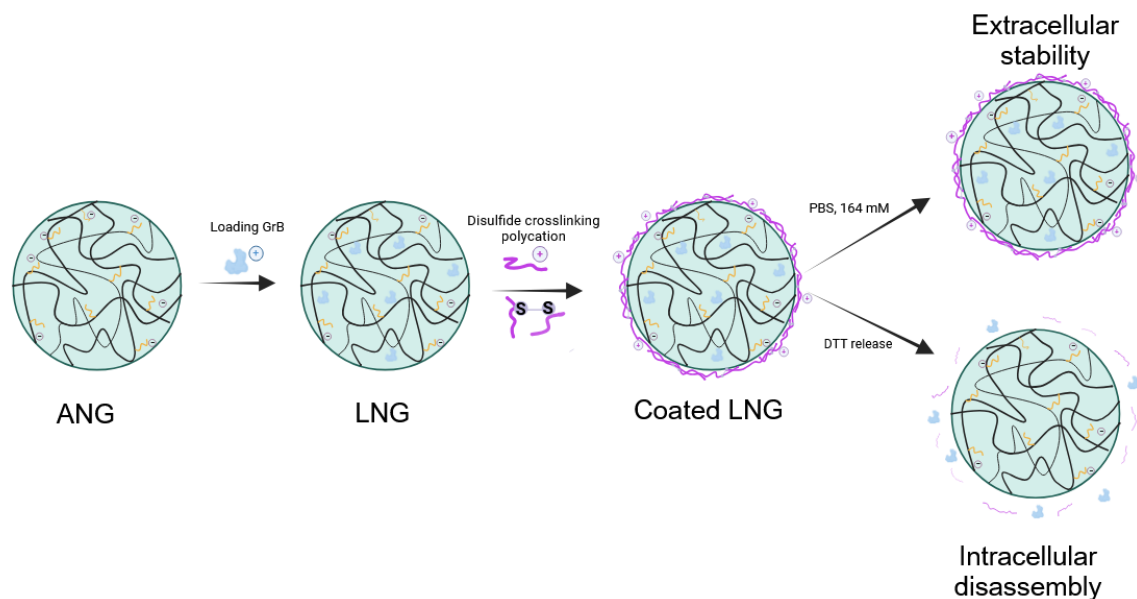


Figure 2. Different layers of the development of the nanogel-based delivery system for Granzyme B (GrB). The process starts with the synthesis of anionic nanogels (ANG)(nanogel synthesis). Positively charged GrB is then post-loaded into the nanogel via electrostatic interactions (loading). These GrB-loaded nanogels (LNG) are coated with a polycation containing protected thiols (coating). Following deprotection, disulfide cross-links are formed, stabilizing the system in physiological conditions. These disulfide bonds are reduced in the intracellular environment, triggering release of GrB (release).

3. Methods

3.1 Materials

Unless otherwise noted, all chemicals were purchased from Sigma-Aldrich and were used according to the manufacturer's instructions. Granzyme B was obtained from UMC Utrecht. Predecessors of this research synthesized methacrylated dextran with a degree of substitution of 8 (Dex-Ma DS 8) and N-(2-hydroxypropyl) methacrylamide (HPMA). Solvents used: Cetyl PEG/PPG-10/1 Dimethicone (ABIL EM 90) was purchased from Goldschmidt; Acetonitrile, acetone and n-hexane were purchased from Biosolve. The buffers used were (4-(2-hydroxyethyl)-1-piperazineethanesulfonic acid) (HEPES, pH 7.4, Acros Chemical), Phosphate buffered saline (PBS, Braun), 2-Morpholinoethanesulphonic acid (MES). Fluorescence dyes, cyanine3 NHS ester and cyanine5 NHS ester, were obtained from Invitrogen.

3.2 Synthesis and characterization of anionic nanogels

Anionic nanogels (ANG) were prepared by inverse emulsion photo-polymerization. For this, 120 mg methacrylated dextran with a degree of substitution of 8 (dex-MA DS8) and 225 μ L Sodium Methacrylate (NaMA) were dissolved in 135 μ L of 1M HEPES or de-ionized water. To enable photo-polymerization, 120 μ L lithium phenyl-2,4,6-trimethylbenzoylphosphinate (10 mg/mL) was added. For the external phase, 4.5 mL of light mineral oil was combined with 0.5 mL ABIL EM 90. Both the internal and external phases were flushed with nitrogen gas. The two phases were emulsified, ultra-sonicated, and polymerized under UV-light for 15 min at 365 nm. The polymerized particles were purified with 5 washing steps using a 1:1 mixture of acetone:hexane. After each washing step, the purified particles were collected by centrifugation. Following the final centrifugation, the product was lyophilized. The obtained nanogels (dispersed in HEPES buffer (20 mM, pH 7.4)) were analyzed with dynamic light scattering (DLS, Malvern Zetasizer nanoseries LB026 nano-s) to determine particle size and polydispersity, and Zetasizer (Malvern Zetasizer nanoseries LB027 nano-z) was used to measure their zeta potential.

3.3 Protein loading

Lysozyme solution (800 μ g/mL) was mixed at a 1:1 volume ratio with nanogel suspension (2 mg/mL) in HEPES 20 mM (pH=7.4). The mixture was left stirring for 1 h and then centrifuged at 15,000 rpm for 1 h to remove the unloaded lysozyme. The concentration of lysozyme in the supernatant was analyzed by Micro-BCA assay. For the loading of GrB into the nanogel, the nanogel was dissolved in HEPES 70 mM (pH=7.4) to a concentration of 0.5 mg/mL. The nanogel and GrB solution (200 μ g/mL) were added in a 1:1 volume ratio. The mixture was left stirring for 1 h and then centrifuged at 15000 rpm for 1 h to remove the unloaded GrB. The concentration of GrB in the supernatant was analyzed by UPLC. The loading efficiency (LE) is calculated by the difference between the added protein concentration and the protein concentration in the supernatant. The formula for LE is

$$LE\% = \frac{[Protein]_{added} - [Protein]_{supernatant}}{[Protein]_{added}} \times 100 .$$

To characterize the resulting pellet's loaded nanogels, the pellet is resuspended in HEPES 20 mM (pH=7.4), and tip sonicated at 10% amplitude for 10 seconds (Bandelin sonoplus UW 2200 – 3mm probe). The size and surface charge of the loaded nanoparticles are measured with DLS and Zetasizer.

Different nanogel-to-lysozyme weight ratios (4.0:1.0, 2.5:1.0, 1.0:1.0, 1.0:2.5) and stirring effect were studied to optimize LE. ANG suspension (2 mg/mL in 20 mM HEPES buffer, pH 7.4) was prepared a day in advance, and lysozyme solution (2 mg/mL in 20mM HEPES buffer, pH 7.4) was prepared fresh on the day of loading. The lysozyme solution and nanogel suspension were diluted, mixed at specified loading ratios and stirred for 3 h (except for sample D). After the samples were centrifuged (1 h 15,000 rpm), LE was determined by analyzing the supernatant, and loaded particles were characterized as described above.

3.3a Protein content determination by Micro-BCA assay

The collected supernatant after each centrifugation was analyzed with Micro-BCA assay to detect the unloaded protein concentration. Standards were prepared by dissolving lysozyme in HEPES 20 mM pH 7.4 in a 1.25-100 µg/mL range. In each well, 150 µL of standard or supernatant, diluted to 33.33 mg/mL (estimated concentration if there was no loading) was pipetted in triplicates. Subsequently, 150 µL of working reagent is added to all the filled wells. The plate is then incubated at 37°C for 2 h, and absorbance is measured at 562 nm with a wellplate reader (BMG LABTECH SPECTROstar nano) to determine the protein concentration in the supernatant.

3.3b Protein content determination by UPLC

The collected supernatant after each centrifugation was analyzed with UPLC to detect the unloaded protein concentration. The UPLC (Acquity UPLC, Waters Corporation, Milford, USA) had a CSH C18 1.7 µm column. Solvent mixtures of 100% H₂O/5% ACN/0,01% perchloric acid and 100% ACN/0.01% perchloric acid were used as eluent A and B, respectively. A flow rate of 1.0 mL/min was used. The injection volume was 10.0 µL, and the protein detection wavelength was 220 nm. The standard curve was prepared by dissolving the protein in HEPES 20 mM pH 7.4 and was linear between 0 to 200 µg/mL protein concentration.

3.4 Synthesis and characterization of cationic polymer coating

3.4a Synthesis of pyridyl disulfide incorporated-polycation (PD-PC)

The pyridyl-disulfide incorporated-polycation (PD-PC) was prepared by functionalizing methacrylic acid copolymer (PC-MAA) with pyridine dithioethylamine HCl (PDEA) via an amidation reaction. 4-(4,6-Dimethoxy-1,3,5-triazin-2-yl)-4-methylmorpholinium Chloride (DMTMM) was used as the coupling reagent. This reaction was done under multiple conditions, with variations in parameters such as amine addition order, reaction temperature and pH of the 2-Morpholinoethanesulphonic acid (MES) buffer. The precipitates were filtered

out, and PD-PC was purified via dialysis (5 times). PD-PC was then collected by lyophilization. The conversion of MAA groups was quantified by adding an excess of dithiothreitol (DTT) and measuring UV-Vis absorbance from the release of 1-Mercaptopyrindine at 344 nm. ^1H NMR (D_2O) was used to quantify the theoretical molecular weight and the amidation by studying the integrals of aromatic protons relative to the rest of the polymer. Gel permeation chromatography (GPC) was used to analyze the molecular weight of the synthesized polymer.

3.4b Synthesis of ATAA incorporated polycation (ATAA-PC)

For the preparation of the ATAA-incorporated polycation coating (ATAA-PC), the co-polymer (CP) was first synthesized. Two monomers, aminoethyl methacrylate hydrochloride (AEMA) and N-(2-hydroxypropyl) methacrylamide (HPMA), were combined into a mixture together with 4-Cyano-4-[(ethylsulfanylthiocarbonyl)sulfanyl]pentanoic acid (CETSP), 2,2'-Azobis[2-(2-imidazolin-2-yl)propane]dihydrochloride (VA-044) and trioxane. The mixture was filled to a final reaction volume of 2 mL with 30% methanol (pH 4.4). The solution was sparged for 20 minutes with nitrogen gas. Afterward, the reaction was left to polymerize while continuously stirred overnight at 45°C in an oil bath. The product was dialyzed against water (4 times) and freeze-dried.

Then the CP is functionalized with 2-(acetylthio)acetic acid (ATAA) through an amidation reaction using DMTMM as the coupling reagent, to produce the final polycation coating, ATAA-PC. In-depth, a mixture of DMTMM and ATAA dissolved in 100 mM MES buffer (pH 5.5) is prepared and, the CP solution is prepared in the same buffer. After 2 h, the DMTMM and ATAA mixture is added to the CP solution. This is left to stir for 3 days at room temperature, purified via dialysis, and finally freeze dried. ^1H NMR (D_2O) was used to quantify the theoretical molecular weight and the amidation by studying the integrals of aromatic protons relative to the rest of the polymer (Table S2 in Supporting Information). GPC measurements were also done to quantify the number average molecular weight of the synthesized polymer.

3.5 Coating of anionic nanogel with cationic polymer

Both nanogel and cationic polymer were dissolved in HEPES 20 mM to a concentration of 2 mg/mL a day in advance. The next day, 0.5 mL of the nanogel and 0.5 mL polycation solutions were mixed. The mixture is incubated for 1 h at room temperature. The size of the obtained coated nanogels was analyzed with DLS, and the zeta potential was measured with Zetasizer.

3.6 Cross-linking of coated anionic nanogel

To cross-link the coated nanogel, 100 μL of deacetylation solution is added to 1.0 mL coated nanogels. Two conditions of the deacetylation standards were tried: one (1 mL HEPES buffer + 789.3 mg hydroxylamine (HA) 50% aqueous solution) and two (1 mL HEPES buffer+ 3.4 mg HA50%). The mixture of coated nanogel and deacetylation solution is left to incubated for 2 h at room temperature to allow the cross-linking reaction to proceed.

3.7 In vitro release from coated nanogels

Coated and lysozyme-loaded nanogels were dispersed in 20 mM HEPES pH 7.4. The samples were centrifuged (15,000 rpm, 1 h) to collect the pellet, which was then resuspended in PBS (164 mM). This washing step with PBS is repeated. The supernatant is collected after each centrifugation to determine free protein concentration via UPLC. Lastly, DTT was added to the 1 mL pellet to a final concentration of 10 mM to trigger the release of the loaded lysozyme. The samples were centrifuged (15,000 rpm, 1 h), and the supernatants were analyzed for released lysozyme concentration with UPLC.

3.8 Fluorescence Correlation Spectroscopy study

Sharad Mohan synthesized the labeled nanogels (Cy5-NG). To label the nanogel, first nanogels were synthesized with a monomer that contained a methacrylate function and a terminal amine group that would react with cyanine5 (Cy5) NHS ester to form an amide bond. In-depth, 120 mg Dex-MA DS 8 in 225 mL dissolved in NaMA (2M) and a solution of 120 mg/mL of N-(4-(2-(pyridine-2-ylidysulfanyl) ethyl)-amido butyl) methacrylamide was dissolved in 1:1 volume ratio of DMSO:Water. To this solution, 135 μ L of HEPES buffer 1M was added, and the mixture was left stirring overnight. To initiate photo-polymerization, 120 μ L LAP (10mg/mL) is added. The dextran solution is then emulsified in the external phase (4.5 mL of light mineral oil containing 0.5 mL ABIL EM 90) by ultra-sonication. Subsequently, the emulsified nanoparticles were polymerized by UV light for 15 minutes, purified by washing with acetone/hexane (50:50 v/v), rehydrated and collected by freeze-drying. After formulating these anionic nanogels, Cy5 NHS ester (1 mg/mL in DMSO) was added to the nanogel solution (5 mg/mL) and left stirring overnight. The solution was dialyzed against pure water (3 times), and Cy-NG 5 was collected via lyophilization.

For labeling GrB, a 0.923 mg/mL GrB solution in 150 mM HEPES pH 7.4 20 mM NaCl was obtained from our collaborators (Laura Priego González, UMC Utrecht). The pH of the solution was adjusted to 8.15 with 1 M NaOH. The GrB solution was then diluted to a final volume of 1 mL with water, and Cy3 NHS ester stock was added to it. This was covered in foil and left to react overnight at 4°C. The next day, the solution was dialyzed against water (4 times) and freeze-dried to collect the labeled GrB (Cy3-GrB).

To label the polymer coating, the polymer was dissolved in 1 M NaHCO₃ and water (pH 7.65). Then, Cy7 NHS ester (0.18 mg/mL in DMSO) was combined with the polymer solution. This was covered in foil and left to stir overnight at 4°C. The solution was then dialyzed against DMSO and water (volume ratio 1:1), then pure water (4 times). The labeled polymer was collected by lyophilization. The diffusion of GrB (free and loaded in nanogel) was measured via fluorescence correlation spectroscopy (Leica Stellaris 8 Fluorescence Microscope). Protein and loaded nanoparticles were prepared in 20 mM HEPES buffer to a final concentration of 1 nM (100 μ L).

4. Results and discussion

4.1 Synthesis and Characterization of Anionic Nanogel

Granzyme B (GrB, 28.5 kDa) has an estimated isoelectric point between 9 and 12; thus, it is positively charged at physiological pH (7).^[14] Hence, anionic nanogels were required to achieve electrostatic loading of GrB. These were synthesized via inverse mini-emulsion photopolymerization. The methacrylated dextran used for the synthesis had a degree of substitution of 8. These nanogels were negatively charged by incorporating an anionic methacrylate monomer, sodium methacrylate (NaMA) to mediate the post-loading of GrB via electrostatic interactions. For the synthesis of dextran nanogels, two nanogel formulations were prepared, one with de-ionized water (ANG1) and one with HEPES buffer (ANG2). This was done to investigate the effect of residual HEPES after washing. HEPES can increase ionic strength and could interfere with protein loading. The yield difference between the two nanogels was 36.3mg, close to the amount of added HEPES, indicating that HEPES is not fully removed in the washing steps during synthesis.

As shown in Table 1, both nanogel formulations had a mean particle size of around 176 nm with a PDI of 0.21, indicating uniform size distribution and stable colloidal properties. The zeta potential was also measured as -35 mV for all formulations. Previously synthesized nanogel by Laura Priego González (HEPES buffer as solvent in internal phase of nanogel, ANG3) had a similar size and zeta potential, confirming the reproducibility of anionic nanogel synthesis.

Table 1. Characterization of the different types of anionic nanogels. Z-average hydrodynamic diameter (Z-ave), polydispersity index (PDI) and zeta potential (ZP).

Sample	Internal phase solvent	Z-ave (nm)	PDI*	ZP (mV)
ANG1	DI-water	175	0.21	-35
ANG2	HEPES 1M	176	0.23	-35
ANG3	HEPES 1M	137	0.18	-31

*PDI < 0.3 is ideal for polymer formulations.

After a month, the nanogels were resuspended in 20 mM HEPES buffer. Both ANG2 and ANG3 showed no change in their size, and no visible aggregation was observed, suggesting excellent stability. In contrast, ANG1 changed drastically in size, and noticeable precipitation was observed, indicating poor stability. This observation correlates with the lower ionic strength of the synthesis solution (di-ionized water). Based on these results, ANG3 was used in further experiments during this research project.

4.2 Loading efficiency of protein in nanogel

This study investigated whether the synthesized nanogels could load protein and quantify the loading efficiency (LE). Predecessors of this project previously determined that the loading efficiency was around 90%. The first loading experiments used lysozyme as a model protein, and LE was analyzed via Micro-BCA. Lysozyme was chosen because it possesses properties like GrB, such as a positive charge (pI= 11.35) at physiological pH; it is commercially available and inexpensive compared to GrB. Although ANG1 showed signs of instability after 1 month, ANG1 and ANG2 remained stable when the micro-BCA loading experiments were done. The loaded ANG1 showed the highest LE=84% among all loaded samples (LNG1, Table 2). This suggests that the residual HEPES influences the loading of protein. However, the results from the Micro BCA assay were inconsistent (Table S1 in Supporting Information). To overcome this, a switch was made to UPLC, which provided more consistent LE measurements. LE was determined via UPLC analysis of the protein concentration of the supernatant. This analysis measured a LE of 39% for the GrB-loaded nanogel (LNG3). As listed in Table 2, the zeta potential of the LNG3 remained negative (-21 mV) after protein loading, and the size did not change after loading (143 nm). These results suggest that GrB was encapsulated within the ANG instead of adsorbed on the surface.

Table 2. Characterization of loaded nanogels. Z-average hydrodynamic diameter (Z-ave), polydispersity index (PDI), zeta potential (ZP), and loading efficiency (LE).

Sample	Protein	Method	Z-ave (nm)	PDI	ZP (mV)	LE(%)
LNG1	Lysozyme	Micro-BCA	209	0.11	-21	84
LNG2	Lysozyme	Micro-BCA	150	0.15	-21	29
LNG3	GrB	UPLC	143	0.28	-18	39

Different nanogel-to-protein loading ratios and the effect of stirring during loading were studied to optimize the LE. The results showed that increasing the nanogel to protein ratio (4.0:1.0) decreased the LE to 67% (Table 3). In contrast, a higher protein-to-nanogel ratio (1.0:2.5) relatively increased the LE to 97. However, these loaded nanogels seemed more likely to aggregate (Z-ave= 7,712 nm). These findings contradicted the expectation that a higher nanogel-to-protein ratio would provide sufficient space and charge for encapsulation, increasing the LE. Instead, the optimum ratio for a high LE with minimal aggregation was found to be in the range of 1.0:1.0 to 2.5:1 nanogel-to-protein ratio (Figure 3). In addition, a higher LE was observed when the nanogel protein mixture was left stirred during loading (LNG3C and LNG3D showing LE of 92.45% and 89.61%, respectively). However, this difference was not significant.

Table 3. Characterization of nanogel samples at varying ANG3 to protein loading ratio. Z-average hydrodynamic diameter (Z-ave), polydispersity index (PDI), zeta potential (ZP), and loading efficiency (LE).

Sample	Ratio (ANG3:Lysozyme)	Weight ratio(ANG3 mg: Lysozyme mg)	Z-ave (nm)	PDI	ZP (mV)	LE (%)
LNG3A	4.0: 1.0	1.6: 0.4	155	0.11	-20	67
LNG3B	2.5: 1.0	1.0: 0.4	147	0.13	-19	76
LNG3C	1.0: 1.0	0.4: 0.4	193	0.15	-15	92
LNG3D*	1.0: 1.0	0.4: 0.4	175	0.14	-16	90
LNG3E	1.0: 2.5	0.4: 1.0	7712	0.42	5	97

*Sample LNG3D was prepared without stirring during loading.

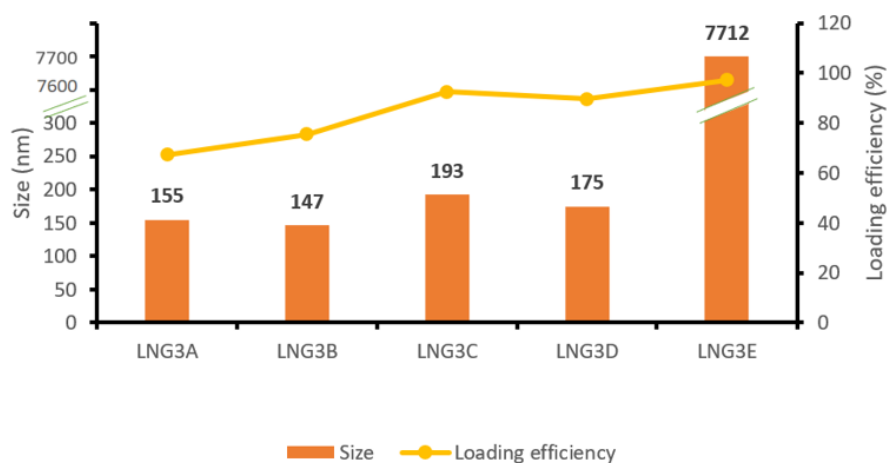


Figure 3. Particle size (Z-ave) and loading efficiency (LE) in relation to different nanogel to lysozyme ratios. LE was measured by UPLC as described in methods.

4.3 Cationic polymer synthesis and characterization after coating nanogel

To release the GrB into the tumor cell, it must stay stably encapsulated in the nanogel and only get released once it reaches the desired intracellular reductive environment. This can be achieved by coating the GrB-loaded nanogel with a reductive sensitive polycation. Two approaches were studied to synthesize cationic polymers: the pyridyl disulfide incorporated-polycation (PD-PC) and the 2-(acetylthio)acetic acid incorporated-polycation (ATAA-PC). In the first approach, PD-PC was prepared with pyridyl disulfide methacrylate acid monomer (PDMAM), which enables cross-linking and the formation of a polymer shell around the nanogels. The PD-PC synthesis involved functionalization of a copolymer containing methacrylate acid residues (PC-MAA copolymer) with pyridine dithioethylamine HCl (PDEA) via an amidation reaction, using Dimethoxy-1,3,5-triazin-2-yl)-4-methylmorpholinium Chloride (DMTMM) as coupling reagent (Scheme 1A). Multiple conditions for DMTMM activated amide coupling were evaluated to find the optimal reaction parameters (Table 4).

Scheme 1. Schematic route for synthesis of cationic polymers coating.

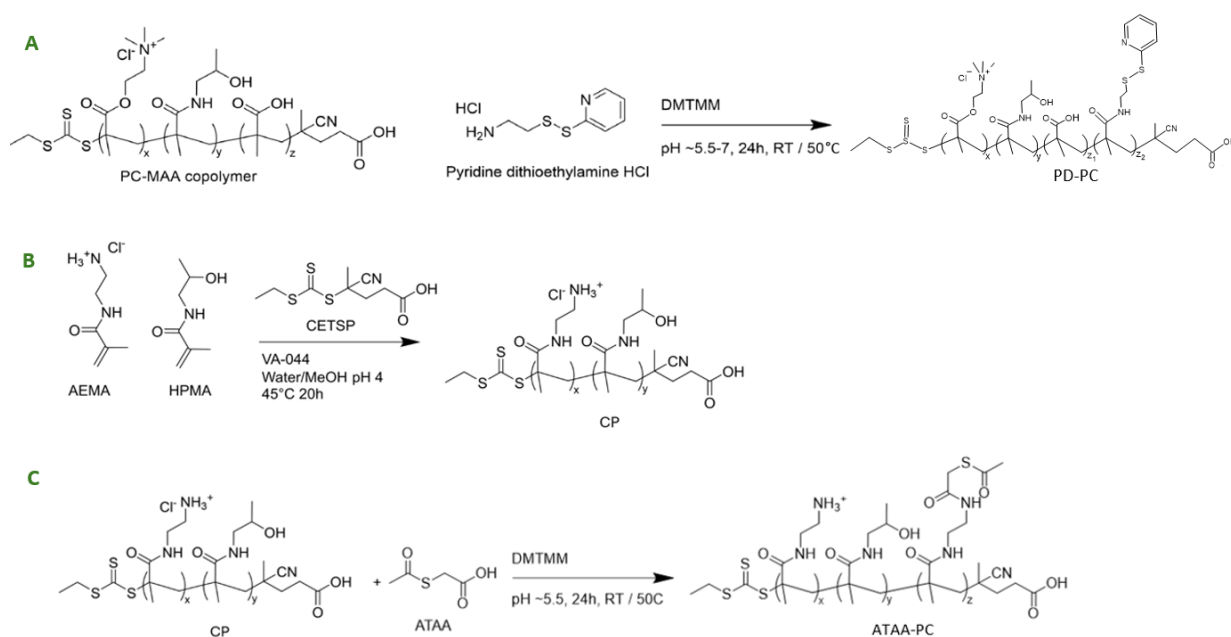


Table 4. Reaction conditions for PD-PC synthesis via DMTMM activated amide coupling. Conditions varied in buffer pH, reaction time, amine addition order and temperature.

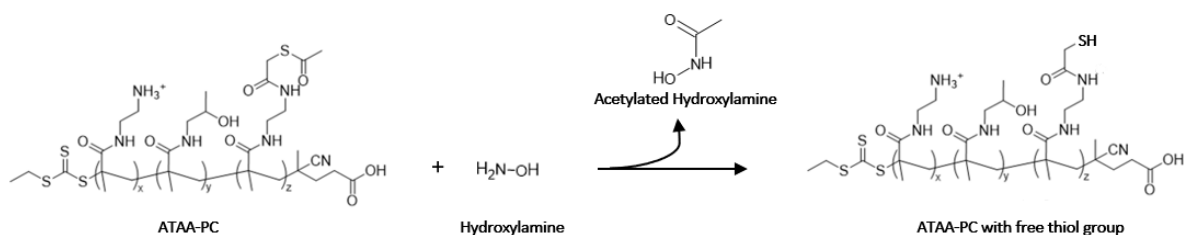
Sample	Buffer (pH, ionic strength)	Time (h)	Addition order and temperature/pH change
PD-PC1	MES (5.5, 100 mM)	24	Add amine after 2 h, 50°C
PD-PC2	MES (6.0, 100 mM)	24	Add amine after 2 h, 50°C
PD-PC3	MES (5.5, 100 mM)	72	Add amine after 2 h, RT
PD-PC4	MES (6.0, 100 mM)	72	Add amine after 2 h, RT
PD-PC5	MES (5.5, 100 mM)	72	Add amine after 2 h, RT, pH 7

UV-vis analysis showed that PD-PC3 demonstrated the best functionalization, achieving a 21% conversion of MAA groups and incorporating approximately 10 PDMAM units per chain, which was sufficient for cross-linking. This corresponds to a 2.5 mol% of PDMAM in the final cationic polymer composition. ^1H NMR measured a theoretical molecular weight ($M_{n,\text{nmr}}$) of 69.1 kDa. Similarly, GPC detected a M_n of 71.5 kDa. Based on these results, the optimal conditions for DMTMM- coupling were determined to be a buffer of pH 5.5, a reaction time of 72 h at room temperature, and a delayed amine addition after 2 h.

However, PD-PC showed some challenges, such as insolubility in HEPES buffer after brief storage at room temperature. This could be due to the formation of cross-links, rendering them unusable to coat the nanogels. Additionally, there was a low molar fraction of protected thiol in the final product. This could be optimized by incorporating more methacrylic acid (MA) residues in the copolymer. However, increasing MA residues could result in polymerizing a polyanion due to the negatively charged MA residues.

To overcome these problems, a second approach was investigated with the focus on a different thiol chemistry. Specifically, thio-ester (ATAA) was used as a protected thiol group, which could later be deprotected by using a deacetylation solution (Scheme 2). ATAA-PC was synthesized by co-polymerizing N-(2-hydroxypropyl) methacrylamide (HPMA), a neutral monomer; aminoethyl methacrylate hydrochloride (AEMA), an anionic methacrylate monomer, into a copolymer (CP) (Scheme 1B). Two types of CP were synthesized, one with RAFT and one without RAFT. The CP was then functionalized with ATAA via DMTMM activated amide coupling under the optimized conditions established in the previous study (Scheme 1C).

Scheme 2. Deprotection of sulfhydryl groups in ATAA-PC with reducing agent hydroxylamine to generate free thiol groups.



Two ATAA-PC variants were prepared: ATAA-PC1a, by functionalizing a RAFT-synthesized CP, and ATAA-PC1b by functionalizing a free radical synthesized CP. ^1H NMR findings showed successful functionalization with integrals matching effectively for both variants. The molar fraction of incorporated ATAA in the final polymer composition was 6.7% for both ATAA-PC1a and ATAA-PC1b (Table 5). ATAA-PC1a had a lower M_n calculated by GPC (46.4 kDa) compared to NMR ($M_n=79.2$ kDa), suggesting the influence of non-RAFT processes, as indicated by its

high dispersity ($\mathcal{D} = 1.82$). In contrast, ATAA-PC1b showed a higher molecular weight (M_n , GPC=191.4 kDa) and dispersity ($\mathcal{D} = 1.86$), consistent with non-RAFT polymerization. Unfortunately, when ATAA-PC1b was dissolved in 20 mM HEPES buffer at pH 7.4, precipitation was observed, leading to poor stability.

To optimize the functionalization of ATAA-PC, the effect of increasing the ATAA amount was investigated. Two additional polymers were prepared: ATAA-PC2a, which followed the same method as ATAA-PC1a, and ATAA-PC2, which had 1.5 times more ATAA and DMTMM than ATAA-PC2a. The CP precursor for these variants was synthesized via RAFT polymerization, achieving a conversion of approximately 75%. The M_n values were consistent with monomer conversion, with values of 81.8 kDa ($^1\text{H NMR}$) and 75.9 kDa (GPC), and an acceptable dispersity of 1.55 for a RAFT-synthesized polyamine.

Both ATAA-PC2a and ATAA-PC2b had similar M_n values of around 80 kDa ($^1\text{H NMR}$) and 60 kDa (GPC) (Table 5). Increasing the ATAA amount did not lead to a significant improvement in functionalization, with the degree of substitution reaching 18% for ATAA-PC2a and 15% for ATAA-PC2b. In summary, these results show a higher molar fraction of protected thiol (6.7%) in this second approach compared to the first approach (2.5%), indicating a successful functionalization of ATAA-PC.

Table 5. Overview of molar ratio of AEMA to ATAA, molar weight (M_n), dispersity (\mathcal{D}), molar fraction of protected thiol and degree of substitution of the ATAA-PC variants.

Polymer	AEMA:ATAA (molar ratio)	M_n (GPC, kDa)	M_n (NMR, kDa)	\mathcal{D}	Molar fraction of protected thiol (%) ^a	Degree of substitution (%)
ATAA-PC1a	1.0:0.4	46.4	79.2	1.82	6.7	12
ATAA-PC1b	1.0:0.4	191.4	N/A	1.86	6.7	N/A
ATAA-PC2a	1.0:0.4	80.2	62.1	1.59	10.1	18
ATAA-PC2b	1.0:0.6	80.4	68.8	1.64	8.2	15

N/A $^1\text{H NMR}$ measurement for ATAA-PC1b could not be done due to insolubility problems, and thus degree of substitution could not be calculated. ^{a)} The method of determining molar fraction of protected thiol in the final polymer is described in Table S2 in the Supporting Information.

For further studies, ATAA-PC 1a was used as the polycation to coat the nanogels. DLS measurements showed that both loaded and unloaded coated nanogels, maintained a size of approximately 170 nm (Table 6). The PDI of these coated nanogels were below <0.3, indicating a uniform size distribution. The polycation coating reversed the surface charge of the coated nanogels to a positive zeta potential of 20 mV. These results indicate a successful coating of the polycation onto the nanoparticles.

Table 6. Influence on size and surface charge after nanogels are coated with cationic polymer coating.

Sample*	Z-ave (nm)	PDI	ZP (mV)
ANG	137	0.18	-31
Loaded ANG	147	0.13	-19
Coated ANG	165	0.22	23
Loaded coated ANG	180	0.19	25

*ANG3 was used for nanogel, loading was with lysozyme and coating was ATAA-PC1a.

4.4 In vitro release study

The release study was conducted with three samples: lysozyme-loaded nanogel with non-cross-linked coating (A), lysozyme-loaded nanogel cross-linked using deacetylation condition one (B), and adding lysozyme-loaded nanogel cross-linked using deacetylation condition two (C). The samples were prepared in HEPES 20 mM, then redispersed in PBS 164 mM simulating physiological conditions, and thereafter in dithiothreitol (DTT) (to a final concentration of 10 mM) which simulates the reductive tumoral intracellular environment.

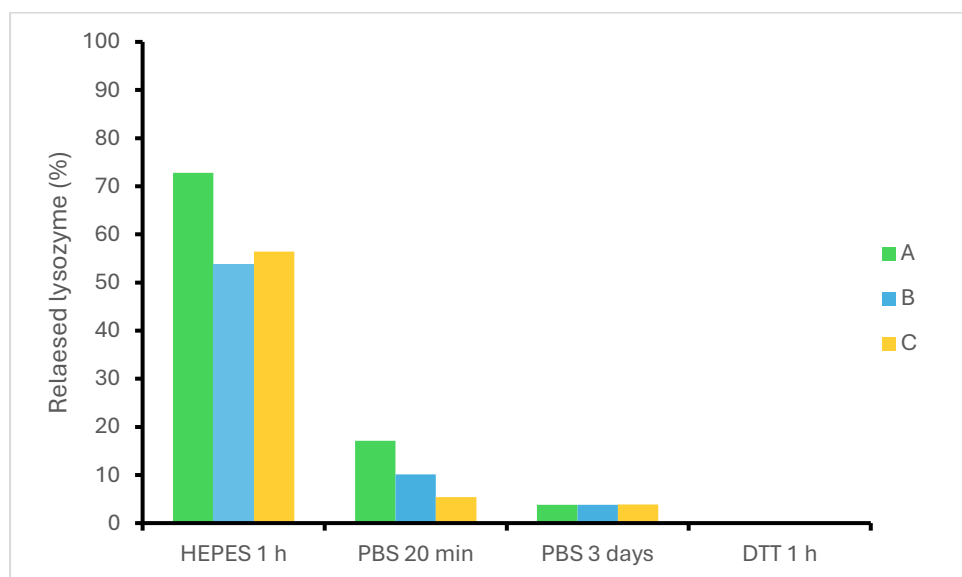


Figure 4. Lysozyme release from nanogel quantified by UPLC. The samples were first dissolved in HEPES 20 mM pH 7.4, then redispersed in PBS 164 mM for 20 minutes and 3 days. Lastly, the nanogels were treated with DTT to a final concentration of 10mM for 1 h.

Figure 4 shows that sample A released the most lysozyme in HEPES. This was expected as these nanogels had a non-cross-linked coating. Samples B and C, with cross-linked coatings, showed less lysozyme release despite expectations that cross-linking would prevent any release. The same trend was observed under physiological conditions, with sample C releasing slightly less lysozyme than B. However, incubation in DTT did not trigger release, contrary to expectations that DTT would cleave the disulfide bonds and cause polymer desorption, releasing the lysozyme. In summary, while deacetylation condition two may be more favorable, the polymer coating seems to be ineffective, as it fails to retain lysozyme under physiological conditions and fails to release lysozyme under reductive conditions. Even under the starting conditions in the HEPES buffer, protein release was observed in all samples. This could be attributed to the relatively low molecular weight of the polycation, which may be absorbed into the nanogel. This absorption could lead to competition for space within the nanogel, subsequently causing the release of the entrapped lysozyme.

4.5 Fluorescence correlation microscopy study

Fluorescence correlation spectroscopy (FCS) was done as a preliminary study to gain a better understanding of the release behavior of GrB from ANG. By analyzing the diffusivity of GrB, FCS enables tracking of GrB and helps determine whether and to what extent GrB stays stored in the ANG after loading or if it gets released. For this study nanogel was labeled with Cy5 (Cy5-ANG), GrB was labeled with Cy3 (Cy3-GrB), and polymer coating was labeled with Cy7. The following samples were prepared: free Cy3-GrB, free Cy5-ANG, Cy3-GrB-loaded Cy5-nanogel, and Cy3-GrB-loaded Cy5-nanogel in 164 nM PBS 24 h.

Unfortunately, several issues arose with the FCS study. Measurement of the loaded nanogel showed signs of crosstalk, making it hard to separate GrB signal and nanogel signal. Labeling the GrB with a different dye like Alexa fluor 350, might reduce crosstalk and improve separating signals. To avoid this, one last measurement was done by loading unlabeled nanogel with Cy3-GrB and comparing it to free Cy3-GrB. In the free Cy3-GrB sample, aggregates were observed, which distorted intensity fluctuations and made it difficult to measure accurate diffusion (Figure S1 in Supporting Information). Only after applying intensive spark filtering to remove the aggregates, a correlation curve with a diffusion coefficient of $56.241 \mu\text{m}^2/\text{s}$ (4 nm) that roughly resembled the size free GrB (2.5 nm) could be obtained. Another underlying cause for these spikes could be due to inconsistent dye labeling of the GrB. Lastly, since aggregated GrB likely cannot enter the nanogel, measuring the loaded nanogel sample was not done. Thus, ensuring GrB stability, having a single dye per particle, and choosing dye with well-separated emission spectra are essential steps for accurate FCS measurement in future experiments.

5. Conclusion

To develop a nanogel-based delivery system for Granzyme B (GrB), anionic nanogels that could encapsulate both lysozyme (as a model protein) and GrB via electrostatic interactions were successfully synthesized. GrB loaded nanogels were optimized to a loading efficiency (LE) of approximately 90%, suggesting that the optimal loading ratio for a high LE with minimal aggregation lies between an ANG:lysozyme ratio of 1.0:1.0 and 2.5:1.0. To keep the entrapped GrB stably stored under physiological conditions, a polycation coating with a good conversion rate (12% mol fraction of ATAA in the final polymer composition) was successfully prepared. In this polycation, the protected thiol groups were deprotected to form cross-links, creating a closed network around the loaded nanogels. However, results from release studies showed that lysozyme loaded nanogel with a cross-linked polycation coating did not retain the lysozyme under physiological conditions and failed to release any lysozyme under reductive conditions. Preliminary results also indicated GrB aggregation in low-salt concentrations.

Further research is needed to investigate alternative polycation synthesis methods and the enhancement of cross-linking efficiency within the coating. Additionally, continued stability testing should be done to ensure GrB stability and activity. Furthermore, studies to investigate the release behavior of loaded GrB from both uncoated and coated nanogels might help to gain valuable insight to optimize the controlled release of the protein.

6. Supporting information

Table S1. Summary of loading efficiency (LE) measurement via Micro BCA assay. Samples were prepared by mixing equal volumes of nanogel suspension with lysozyme solution, both in 20 mM HEPES buffer, pH 7.4. After centrifugation, the supernatant was analyzed using the Micro BCA assay.

Samples	Concentration ANG (mg)	Concentration lysozyme (mg)	Study 1 LE (%)	Study 2 LE (%)
LNG1a	2.0	0.8	83	84
LNG1b	0.5	0.2	70	62
LNG2a	2.0	0.8	52	29
LNG2b	0.5	0.2	71	-8

The results showed inconsistency and unreliability in LE, which could potentially be caused due to variations in sample preparation or the sensitivity limits of the Micro BCA assay.

Table S2. Characterization of cationic polymers by ^1H NMR (D_2O). Polymer structure, degree of substitution (DS) and molar fraction of protected thiol of synthesized polycation in this research project.

Polycation	Polymer structure	DS (%) ^a	Molar fraction of protected thiol (%) ^b
PD-PC3	TMAEMA ₁₉₇ -C-HPMA ₁₅₆ -C-MAA ₃₈ -C-PDMAM ₁₀	21	2.5
ATAA-PC1a	pAEMA ₂₃₄ -C-HPMA ₂₂₇ -C-ATAA ₃₃	12	6.7
ATAA-PC1b	pAEMA _{1.1} -C-HPMA _{1.0} -C-ATAA _{0.15}	N/A	6.7
ATAA-PC2a	pAEMA ₂₂₄ -C-HPMA ₂₁₉ -C-ATAA ₅₀	18	10.1
ATAA-PC2b	pAEMA ₂₃₈ -C-HPMA ₂₁₉ -C-ATAA ₄₁	15	8.2

^a) Degree of substitution (protected thiol units / functionalizable monomer units x 100%); ^b) Molar fraction of protected thiol (protected thiol units/total number of monomer units x 100%); ^c) Mol ratio of structure for ATAA-PC1b; N/A ^1H NMR measurement for ATAA-PC1b could not be done due to insolubility problems, and thus degree of substitution could not be calculated

Additionally, to quantifying functionalization by DS, the molar fraction of protected thiol in the final polymer composition was also calculated. The DS was determined based on the specific functionalizable monomer units, which differed between the two polycation types and had also varied in unit counts. By measuring the functionalization in molar fraction of protected thiol, a more straightforward comparison could be made between PD-PC and ATAA-PC.



Figure S1. Fluorescence Correlation Spectroscopy measurement to track free GrB diffusion. GrB was labeled with Cy3 and resuspended in HEPES buffer (20 mM pH 7.4), to a final concentration of 1 μ M. FCS showed bright, large spots corresponding to GrB aggregates, indicating aggregation under these conditions.

7. References

1. World Health Organization. Cancer. [Internet]. Available from: <https://www.who.int/news-room/fact-sheets/detail/cancer>. [Accessed 23rd Oct 2024].
2. Alberts B, Johnson A, Lewis J, et al. Molecular Biology of the Cell [Internet]. 4th ed. Cancer Treatment: Present and Future. New York: Garland Science; 2002 [Accessed 23rd Oct 2024]. Available from: <https://www.ncbi.nlm.nih.gov/books/NBK26811/>
3. Wang X, Zhang H, Chen X. Drug resistance and combating drug resistance in cancer. *Cancer Drug Resist.* 2019 Jun 19;2(2). DOI: 10.20517/cdr.2019.10.
4. Zitvogel L, Tesniere A, Kroemer G. Cancer despite immunosurveillance: immunoselection and immunosubversion. *Nat Rev Immunol.* 2006 Sep 15;6(10):715–27. DOI: <https://doi.org/10.1038/nri1936>
5. McAllister SS, Weinberg RA. The tumour-induced systemic environment as a critical regulator of cancer progression and metastasis. *Nat Cell Biol.* 2014 Aug 1;16(8):717–27. DOI: <https://doi.org/10.1038/ncb3015>
6. Hargrave A, Mustafa AS, Hanif A, Tunio JH, Hanif SNM. Recent Advances in Cancer Immunotherapy with a Focus on FDA-Approved Vaccines and Neoantigen-Based Vaccines. *Vaccines (Basel).* 2023 Oct 25;11(11):1633. DOI: 10.3390/vaccines11111633.
7. Rallis KS, Corrigan AE, Dadah H, George AM, Keshwara SM, Sideris M, et al. Cytokine-based Cancer Immunotherapy: Challenges and Opportunities for IL-10. *Anticancer Res.* 2021 Jul;41(7):3247–3252. DOI: 10.21873/anticancer.15110
8. Qian X, Shi Z, Qi H, Zhao M, Huang K, Han D, et al. A novel Granzyme B nanoparticle delivery system simulates immune cell functions for suppression of solid tumors. *Theranostics.* 2019;9(25):7616–7627. DOI: 10.7150/thno.35900.
9. Cullen SP, Brunet M, Martin SJ. Granzymes in cancer and immunity. *Cell Death Differ.* 2010 Jan 15; 17:616–623. DOI: <https://doi.org/10.1038/cdd.2009.206>
10. Kashyap D, Garg VK, Goel N. Chapter Four - Intrinsic and extrinsic pathways of apoptosis: Role in cancer development and prognosis [Internet]. In: Donev R, editor. *Advances in Protein Chemistry and Structural Biology*. Academic Press; 2021. p. 73–120. [Accessed 23rd Oct 2024]. Available from: <https://www.sciencedirect.com/science/article/abs/pii/S1876162321000134>
11. Gupta J, Sharma G. Nanogel: A versatile drug delivery system for the treatment of various diseases and their future perspective. *Drug Deliv. and Transl. Res.* 2024 Aug 5;11. DOI: <https://doi.org/10.1007/s13346-024-01684-w>
12. Li D, Kordalivand N, Fransen MF, Ossendorp F, Raemdonck K, Vermonden T, et al. Reduction-Sensitive Dextran Nanogels Aimed for Intracellular Delivery of Antigens. *Adv Funct Mater.* 2015 Apr 8;25(20):2993–3003. DOI: [10.1002/adfm.201500894](https://doi.org/10.1002/adfm.201500894)
13. Li D, Chen Y, Mastrobattista E, van Nostrum CF, Hennink WE, Vermonden T. Reduction-Sensitive Polymer-Shell-Coated Nanogels for Intracellular Delivery of Antigens. *ACS Biomater Sci Eng.* 2017 Jan 9;3(1):42–48. DOI: [10.1021/acsbiomaterials.6b00651](https://doi.org/10.1021/acsbiomaterials.6b00651)
14. Froelich, J. Chapter 598-Granzyme B. [Internet]. In: Rawlings ND, Salvesen G, editors. *Handbook of Proteolytic Enzymes*. Cambridge: Academic Press; 2013, p. 2718–2721. [Accessed 23rd Oct 2024]. Available from: www.sciencedirect.com/science/article/abs/pii/B9780123822192005986.